

fraction, suggesting that the decreased HSPC number and frequency is not attributable to the induction of apoptosis (Figure S2K). In agreement, expression levels of apoptosis-related genes in purified HSCs were not significantly upregulated after c-di-GMP treatment (Figure S2L). By contrast, expression levels of cyclin-dependent kinase inhibitors were consistently decreased in HSCs relative to controls after c-di-GMP treatment (Figure 2M). Collectively, these findings indicate that c-di-GMP treatment induces the entry of HSCs into the cell cycle rather than apoptosis. Importantly, the endogenous STING ligand, cGAMP (Ablasser et al., 2013), elicited HSPC responses less potently than c-di-GMP (Figure S2M), suggesting a c-di-GMP-specific role in anti-microbial defense systems other than cGAS-mediated anti-double-stranded DNA responses.

### c-di-GMP Induces HSPC Expansion in the Spleen

Given that c-di-GMP is potentially an immunostimulatory molecule, we hypothesized that it activates HSPC egress from the BM. We first performed histological observation of the spleen with or without c-di-GMP treatment. As expected, we observed spleen hematopoiesis marked by the presence of megakaryocytes in the red pulp, with slight destruction of the white pulp architecture (Figure 3A). There was a significant increase in spleen weight (Figure S3A) and MPP frequency and number compared with controls (Figures 3B and 3C; data not shown), while HSCs and differentiated cells did not show a significant increase (Figures 3C–3E and S3B–S3D), indicating that c-di-GMP-induced expansion is prominent in MPP fractions. Upon transplantation of splenocytes into lethally irradiated mice, the control group died by day 12, whereas 62.5% of mice transplanted with cells from c-di-GMP-treated mice survived (Figure 3G), indicating that functional HSPCs had been mobilized to the spleen. Intriguingly, however, the long-term reconstitution of purified HSCs did not significantly differ between spleen cells from c-di-GMP-treated and control groups (Figure S3D), in accordance with the comparable number of HSCs between the two groups in the spleen. Use of a larger sample size ( $n = 26$ ) enabled us to detect increases in splenic HSC number following c-di-GMP treatment (Figure S3F). On the other hand, MPPs from c-di-GMP-treated Ubc-GFP reporter mice showed enhanced short-term reconstitution of PB cells, in sharp contrast to BM MPPs (Figures 2K and 3G). The *in vitro* differentiation capacity of single *STING*<sup>+/+</sup> or *STING*<sup>-/-</sup> MPPs did not markedly differ between control and c-di-GMP-treated groups (Figure S3H).

The frequency (Figure S3G) and colony-forming capacity (Figures S3I and S3J) of HSPC fractions also increased in PB after c-di-GMP treatment, suggesting that immature HSPCs are mobilized to the periphery after c-di-GMP administration. However, BrdU analysis showed that CD150<sup>+</sup>CD41/CD48<sup>+</sup> LSK cells in the spleen robustly accumulated BrdU following c-di-GMP

treatment, suggesting that both migration and proliferation underlie the increase in splenic MPPs (Figure S3K).

Of note, cGAMP did not sufficiently increase the number of splenic HSPCs compared to c-di-GMP (Figure S3L).

### c-di-GMP Activates the Irf3/Type I IFN Axis in LT-HSCs through STING

We performed a cDNA microarray followed by gene set enrichment analysis (GSEA) on purified LT-HSCs to examine which pathway is activated following c-di-GMP treatment *in vivo*. IFN- $\alpha$  response genes and Irf3 target genes were significantly enriched in the c-di-GMP treatment group (Figure 4A). Using real-time qPCR, we confirmed that both STING and Irf3 were highly expressed in HSPC fractions, including LT-HSCs, at levels comparable to or even higher than those in BM-derived macrophages (Figure 4B).

In *STING*<sup>-/-</sup> mice, the numbers of HSCs and MPPs were unchanged following c-di-GMP treatment (Figure 4C). In addition, phenotypic HSPC expansion in the spleen was abrogated in c-di-GMP-treated *STING*<sup>-/-</sup> mice (Figure 4D). Thus, the effects of c-di-GMP on HSPCs were entirely dependent upon STING-mediated signaling. To evaluate the contribution of c-di-GMP/STING-dependent signaling to an anti-microbial response, we performed CeLP on *STING*<sup>-/-</sup> mice. MPP expansion in the BM was partially abolished in *STING*<sup>-/-</sup> mice, while the numbers of HSCs in the BM (Figure S4A) and HSPCs in the spleen (Figure S4B) were not restored. We also confirmed insufficient MPP expansion in the BM of *STING*<sup>-/-</sup> mice at day 3 of CeLP (data not shown), indicating that STING-mediated signaling acts primarily on MPP expansion in the BM under bacterial septic conditions.

### The Irf3/Type I IFN Axis Underlies HSPC Expansion in the BM but Does Not Regulate HSPC Mobilization

Our findings indicate that STING is essential for c-di-GMP signaling in HSPCs. Given that STING transduces its signal via Irf3/type I IFN (Crane and Cao, 2014; Ishikawa and Barber, 2008), we treated IFN- $\alpha$  receptor 1 (*Irfar1*)-deficient (*Irfar1*<sup>-/-</sup>) mice with c-di-GMP to determine if treatment stimulated HSPCs in the absence of a type I IFN response. MPP expansion observed in *Irfar1*<sup>+/+</sup> mice was at least partially inhibited in *Irfar1*<sup>-/-</sup> mice (Figure 4E), while the decrease in HSC number seen in *Irfar1*<sup>+/+</sup> mice was not rescued in *Irfar1*<sup>-/-</sup> mice. By contrast, MPPs, which egressed to the spleen upon c-di-GMP treatment in *Irfar1*<sup>+/+</sup> mice, were not reduced in number in the spleen of *Irfar1*<sup>-/-</sup> mice. Surprisingly, phenotypic HSCs, which did not expand in response to c-di-GMP in *Irfar1*<sup>+/+</sup> mice, expanded in the absence of *Irfar1* (Figure 4F), suggesting that type I IFN negatively regulates HSC mobilization in the presence of c-di-GMP.

(K) Five hundred CD150<sup>+</sup>CD41/CD48<sup>+</sup> LSK cells, CD34<sup>+</sup>Flt3<sup>+</sup> LSK cells, or LSK<sup>-</sup> cells from BM MPP fractions of PBS- (Ctrl) or c-di-GMP (cdG)-treated Ubc-GFP mice were transplanted. The frequency of donor-derived cells was assessed 2 (upper panels) and 4 (lower panels) weeks later ( $n = 5$ ).

(L) Cell-cycle status of the indicated HSPC fractions in the BM as measured by Hoechst 33342 and BrdU staining. Percentages of BrdU<sup>+</sup> cells are shown. CD150<sup>+</sup>CD41<sup>-</sup>CD48<sup>-</sup> LSK cells specifically showed an activated cell-cycle status after c-di-GMP treatment (mean  $\pm$  SD,  $n = 5$ ).

(M) Expression of cyclin-dependent kinase inhibitor transcripts (*Cdkn1a*, *Cdkn1b*, *Cdkn1c*, and *Cdkn2a*) in CD150<sup>+</sup>CD41<sup>-</sup>CD48<sup>-</sup>CD34<sup>+</sup>Flt3<sup>-</sup> LSK cells from mice intraperitoneally injected with PBS (Ctrl, open bars) or 200 nmol of c-di-GMP (cdG, closed bars) 3 days before analysis (mean  $\pm$  SEM,  $n = 4$ ). Each value was normalized to  $\beta$ -actin expression and is expressed as the fold induction compared to control group levels.

\* $p < 0.05$  and \*\* $p < 0.01$  compared to PBS-injected control mice. See also Figure S2.

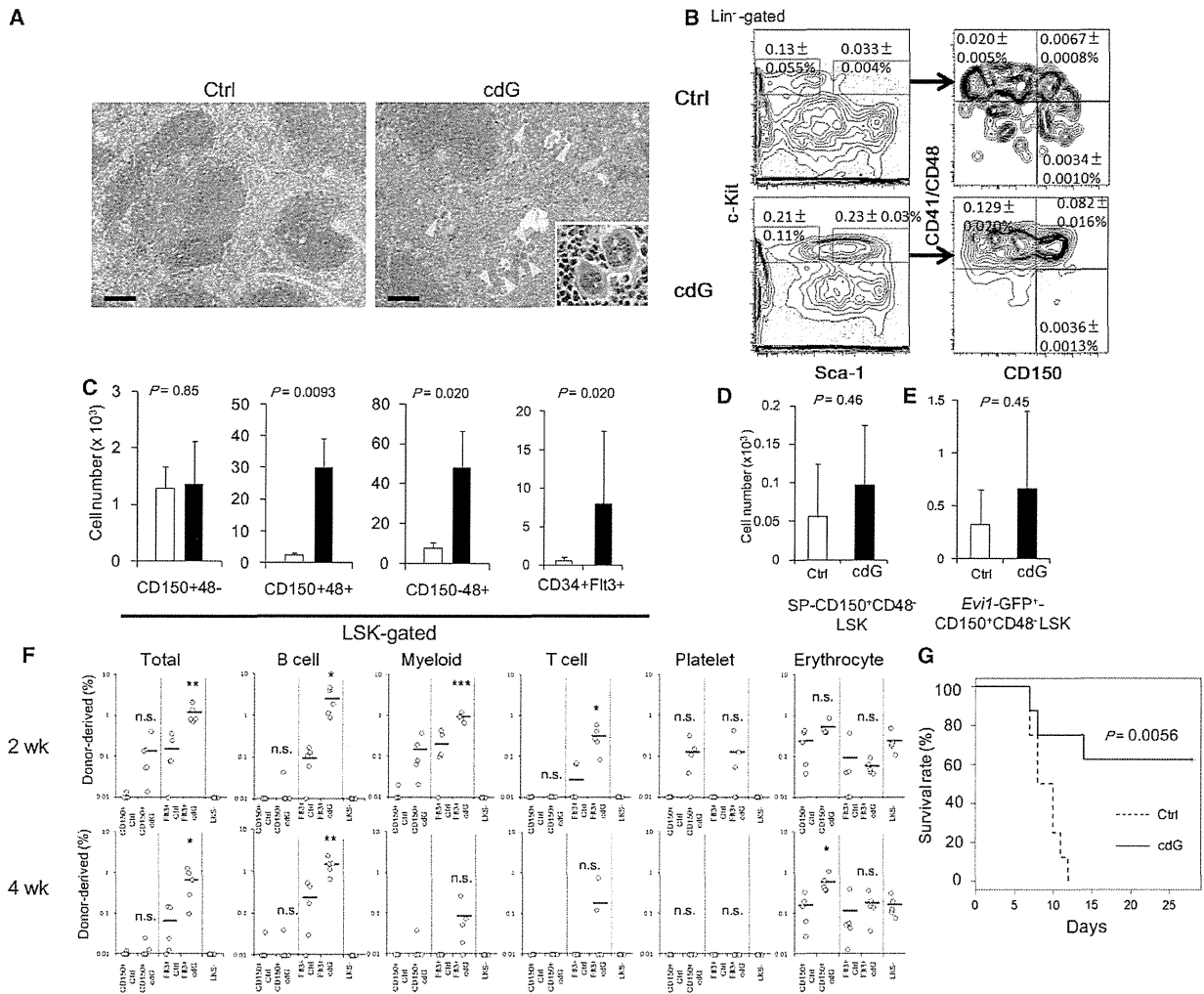


### Figure 3. c-di-GMP Induces the Expansion of Splenic HSPCs

(A) Mice were intraperitoneally injected with PBS (Ctrl) or 200 nmol of c-di-GMP (cdG), and the spleen was stained with H&E. Arrowheads indicate megakaryocytes. A high-magnification image is shown as an inset on the c-di-GMP image. Scale bars indicate 100  $\mu$ m.

(B and C) Mice were injected intraperitoneally with 200 nmol of c-di-GMP (closed bars) or PBS (open bars), and the cell number of each indicated HSPC fraction in the spleen was analyzed 3 days later. (B) Flow cytometric analysis of the splenic HSPC fraction. Representative FACS plots of the Lin<sup>-</sup> fraction and the frequency among whole splenocytes are shown (mean  $\pm$  SD, n = 4). (C) The number of cells in the LSK fractions in the spleen. The number of MPPs (CD150<sup>+</sup>CD48<sup>+</sup> LSK, CD150<sup>-</sup>CD48<sup>+</sup> LSK, and CD34<sup>+</sup>Flt3<sup>+</sup> LSK) increased significantly, while the number of LT-HSCs (CD150<sup>+</sup>CD48<sup>-</sup> LSK) was comparable to that in the control group (mean  $\pm$  SD, n = 4–10).

(D) The number of spleen cells residing in the SP of the SLAM LSK-gated fraction (mean  $\pm$  SD, n = 4).

(E) The number of Evi1-GFP<sup>+</sup> CD150<sup>+</sup>CD41<sup>-</sup>CD48<sup>-</sup> LSK cells in the spleen of PBS- (Ctrl) or c-di-GMP (cdG)-treated mice (mean  $\pm$  SD, n = 4 from two independent experiments).

(F) Five hundred CD150<sup>+</sup>CD41/CD48<sup>+</sup> LSK cells, CD34<sup>+</sup>Flt3<sup>+</sup> LSK cells, or LSK<sup>-</sup> cells from spleen MPP fractions of PBS- (Ctrl) or c-di-GMP (cdG)-treated Ubc-GFP reporter mice were transplanted. The frequency of donor-derived cells was examined 2 (upper panels) and 4 (lower panels) weeks later (n = 5).

(G) Mice were injected intraperitoneally with PBS (Ctrl) or 200 nmol of c-di-GMP (cdG), and  $5 \times 10^5$  spleen cells from each group were transplanted into lethally irradiated (9.5 Gy) mice 3 days later. A Kaplan-Meier survival curve is shown (n = 8); the dashed line indicates the Ctrl group and the solid line indicates the cdG group.

\*p < 0.05, \*\*p < 0.01, and \*\*\*p < 0.001 compared with control mice. ND, not detected. See also Figure S3.

As was seen in *Irfar1*<sup>-/-</sup> mice, the number of phenotypic MPPs in the BM of *Irf3*<sup>-/-</sup> mice did not increase in response to c-di-GMP treatment, while the number of HSCs in the BM was comparable in c-di-GMP-treated *Irf3*<sup>+/+</sup> and *Irf3*<sup>-/-</sup> mice (Figure S4C). Of note,

not only MPPs but also phenotypic HSCs expanded in the spleen of c-di-GMP-treated *Irf3*<sup>-/-</sup> mice (Figure S4D).

*Irf7*, another master regulator of type I IFN signaling (Honda and Taniguchi, 2006), was expressed at comparable levels in

HSPCs and BM-derived macrophages (Figure S4E), and HSCs exhibited a 4-fold increase in *Irf7* expression following c-di-GMP administration (Figure S4F). We tested the effects of c-di-GMP in *Irf3/Irf7* doubly deficient (*Irf3*<sup>-/-</sup>:*Irf7*<sup>-/-</sup>) mice. Similar to observations in *Irf3*<sup>-/-</sup> and *Irf7*<sup>-/-</sup> mice, MPP expansion in the BM was abrogated in *Irf3*<sup>-/-</sup>:*Irf7*<sup>-/-</sup> mice following c-di-GMP treatment (Figure S4G), whereas both phenotypic HSCs and MPPs markedly expanded in the spleen (Figure S4H).

On the other hand, inhibition of NF- $\kappa$ B, another downstream STING target, by the IKK $\alpha$  inhibitor Bay11-7082 almost completely rescued the effects of c-di-GMP, suggesting that NF- $\kappa$ B signaling downstream of c-di-GMP/STING is an important regulator of HSPC behavior (Figures S4I and S4J). Notably, however, c-Kit expression was decreased in c-di-GMP- or Bay11-7082-treated mice (data not shown), making it difficult to accurately determine the number of HSPCs.

### STING Regulates HSPC Homeostasis in the BM and Spleen in Both Cell-Autonomous and Non-Cell-Autonomous Manners

We next asked whether c-di-GMP treatment reduces the sizes of various HSPC fractions (Figures 2C and 2D) directly or indirectly. c-di-GMP is difficult to introduce into cultured cells without lipofection in an ex vivo setting (McWhirter et al., 2009), and HSCs are highly lipofection resistant (Keller et al., 1999); therefore, we used the STING stimulant 10-carboxymethyl-9-acridanone (CMA) (Cavlar et al., 2013), which can freely enter the cytoplasm, to test whether STING stimulation altered HSPC proliferation. To this end, we performed ex vivo colony-forming assays in the presence or absence of CMA using *STING*<sup>+/+</sup> or *STING*<sup>-/-</sup> BMMNCs as well as LSK cells (Figure 5A). The colony-forming capacity of both *STING*<sup>+/+</sup> BMMNCs and LSK cells dose-dependently decreased following CMA treatment, but *STING*<sup>-/-</sup> cells did not exhibit a decrease in CFU in culture (CFU-C) following CMA treatment (Figure 5B). Additionally, the number of high proliferative potential colony-forming cells (HPP-CFCs) dose-dependently decreased following CMA treatment, an effect that was absent in *STING*<sup>-/-</sup> cells (Figure 5C). Unexpectedly, ex vivo treatment of BMMNCs, LSK cells, or LT-HSCs with c-di-GMP also led to dose-dependent decreases in both CFU-Cs and HPP-CFCs (Figures S5A and S5B). This phenotype was also observed in *STING*<sup>-/-</sup> HSCs at higher concentrations (100  $\mu$ M) (Figures S5C and S5D), suggesting that c-di-GMP plays an unknown STING-independent role in this context, which was not observed in vivo (Figure 4B). To confirm the effects of STING-mediated signaling on LT-HSC reconstitution capacity, we incubated sorted *STING*<sup>+/+</sup> or *STING*<sup>-/-</sup> HSCs in culture medium containing CMA for 3 days and then assessed the HSC number. Unlike in comparably treated *STING*<sup>-/-</sup> cells, the number of HSCs significantly decreased among CMA-treated *STING*<sup>+/+</sup> cells (Figure 5D), again revealing an HSPC-autonomous function of STING-mediated signaling. We also treated *STING*<sup>+/+</sup> and *STING*<sup>-/-</sup> HSCs with CMA for 3 days and then transplanted the cells into recipients (Figure 5E). Short-term reconstitution of CMA-treated *STING*<sup>+/+</sup> cells was abrogated, whereas that of *STING*<sup>-/-</sup> cells was not, consistent with the transiently decreased repopulation capacity seen after in vivo c-di-GMP treatment (Figure 2). On the other hand, 16 hr of CMA treatment

did not compromise the HSC repopulation capacity (Figures S5E and S5F), suggesting that short-term exposure is not sufficient to elicit downstream STING signaling in HSCs.

Finally, to test a direct effect of c-di-GMP/STING signaling on HSPCs in vivo, we performed reciprocal transplantations, in which the BM of *STING*<sup>+/+</sup> recipients was replaced with *STING*<sup>+/+</sup> or *STING*<sup>-/-</sup> donor cells (Figures 5F–5H) and the BM of *STING*<sup>+/+</sup> or *STING*<sup>-/-</sup> recipients was replaced with *STING*<sup>+/+</sup> donor cells (Figures 5I–5K). In agreement with the results of CMA experiments, the number of *STING*<sup>-/-</sup> donor HSCs in *STING*<sup>+/+</sup> recipients did not decrease following c-di-GMP administration (Figure 5G) and splenic MPPs did not increase (Figure 5H), suggesting a cell-autonomous effect of c-di-GMP on HSPCs. Likewise, the number of *STING*<sup>+/+</sup> donor HSCs in *STING*<sup>-/-</sup> recipients did not decrease (Figure 5J) and HSPC expansion in the spleen was abrogated following c-di-GMP treatment (Figure 5K). Collectively, in addition to cell-autonomous activity, STING controls the HSPC pool size in the BM and spleen in a non-cell-autonomous manner. To further test the cell-autonomous effects of c-di-GMP on HSPCs, we established chimeric mice whose BM contained a 1:1 ratio of *STING*<sup>+/+</sup> and *STING*<sup>-/-</sup> cells and treated them with c-di-GMP (Figure S5G). Following treatment, BM chimerism of *STING*<sup>-/-</sup> donor-derived myeloid and B cells was decreased, suggesting that, in addition to its direct impairment of HSC function, the cell-autonomous and non-cell-autonomous effects of c-di-GMP treatment favor myeloid and B cell production, presumably through the migration of MPP cells to the periphery (Figure S5H).

### c-di-GMP Attenuates the Niche Function of Mesenchymal Stromal Cells in BM

We next sought to define the mechanisms underlying HSPC egress from the BM. HSCs reside in specialized BM niches that regulate the balance between self-renewal and differentiation, and the ablation of niche cells promotes loss of quiescence and HSC mobilization (Méndez-Ferrer et al., 2010), effects comparable to those observed following c-di-GMP administration. BM architecture was drastically changed by c-di-GMP treatment, with a massive decrease in cellularity and an increase in the size of the sinusoidal area surrounded by PLVAP<sup>+</sup> endothelial cells (Figures 6A–6C). This change in sinusoidal architecture was also observed in *Irf3*<sup>-/-</sup>:*Irf7*<sup>-/-</sup> mice, and *STING*<sup>-/-</sup> BM chimeric mice, whereas *STING*<sup>-/-</sup> mice showed no structural changes (Figure S6A), suggesting a STING-dependent *Irf3/Irf7*-independent effect of c-di-GMP on non-hematopoietic cells. These changes motivated us to examine the frequency and number of several types of HSPC niche cells that reportedly reside in the BM, including endothelial cells, osteoblastic progenitor cells, and mesenchymal stromal cells (MSCs) (Pinho et al., 2013), which essentially overlap with CXCL12-abundant reticular cells (Omatsu et al., 2010) and CD45<sup>-</sup>Ter119<sup>-</sup>LepR<sup>+</sup> cells (Zhou et al., 2014). Every non-hematopoietic niche cell type showed a significant decrease in both frequency and number after c-di-GMP treatment (Figures 6D and 6E), suggesting that deformation of multiple niche components promotes HSPC detachment from the BM.

Among BM non-hematopoietic cells, platelet-derived growth factor receptor (PDGFR) $\alpha$ <sup>+</sup> integrin  $\alpha$ V (CD51)<sup>+</sup> MSCs

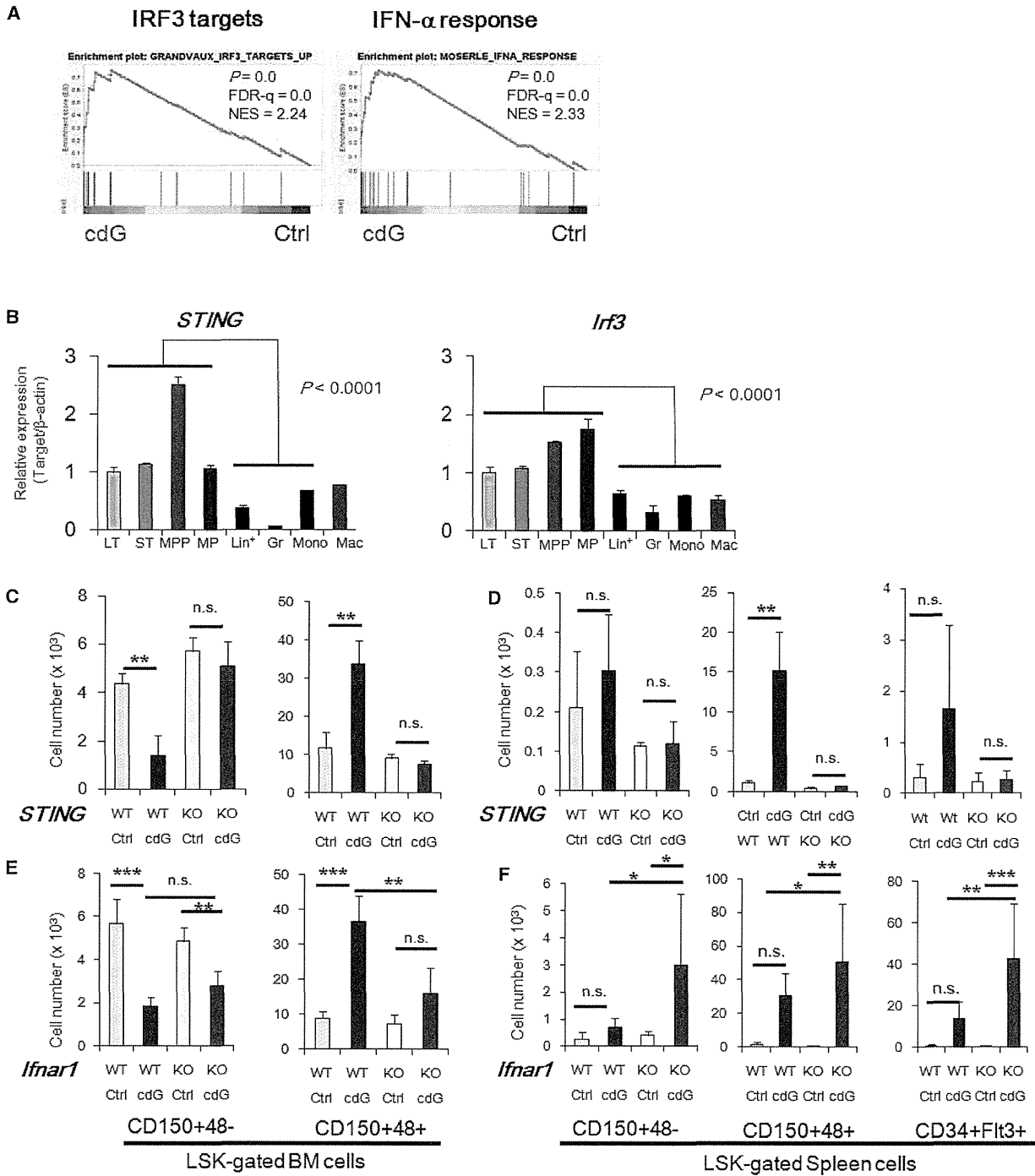


**Figure 4. Type I IFN Activity Is Partially Responsible for HSPC Expansion but Inhibitory to Phenotypic HSPC Expansion in the Spleen**  
 (A) GSEA was performed using cDNA microarray data of CD150<sup>+</sup>CD41<sup>-</sup>CD48<sup>-</sup>CD34<sup>-</sup>Fit3<sup>-</sup> LSK cells from PBS- or c-di-GMP-treated mice. Results for an Irf3 downstream target gene set and an IFN- $\alpha$  responsive gene set are shown. FDR-q, false discovery rate. NES, normalized enrichment score.  
 (B) Expression levels of STING (left) and Irf3 (right) in the indicated hematopoietic fractions, including LT-HSCs (CD34<sup>-</sup>Fit3<sup>-</sup> LSK, LT), short-term HSCs (CD34<sup>+</sup>Fit3<sup>-</sup> LSK, ST), multipotent progenitors (CD34<sup>+</sup>Fit3<sup>+</sup> LSK, MPP), myeloid progenitors (Lineage<sup>-</sup>c-Kit<sup>+</sup>Sca-1<sup>-</sup>, MP), lineage-marker-positive cells (Lin<sup>+</sup>), granulocytes (Gr-1<sup>+</sup> Mac-1<sup>+</sup>, Gr), monocytes (Gr-1<sup>-</sup> Mac-1<sup>+</sup>, mono), and BM-derived macrophages (Mac), were analyzed by qPCR. Each value was normalized to  $\beta$ -actin expression and is expressed as the fold difference compared to levels in LT-HSC samples (mean  $\pm$  SD, n = 4).  
 (legend continued on next page)

expressed the highest levels of *STING* and *Irf3* (Figure 6F), suggesting that, in addition to hematopoietic cells, MSCs are a primary target of STING-mediated signaling, and that the decrease in the number of other cell types could be ascribed to non-cell-autonomous mechanisms. We then quantified the expression levels of specific factors that maintain HSC function or anchor cells to the niche in sorted niche cells upon c-di-GMP treatment. KitL, CXCL12, Angpt1, and VCAM1 expression levels invariably decreased following the treatment of MSCs (Figure 6G). Importantly, MSC expression of factors that maintain HSPCs was lower in c-di-GMP-treated *Irfnar1*<sup>-/-</sup> mice than in similarly treated controls (Figure 6G). This result indicates that c-di-GMP treatment attenuates HSPC maintenance and anchoring in the BM niche and that the underlying mechanism is type I IFN independent. HSCs co-cultured with CMA-treated OP9 cells showed a dose-dependent decrease in colony number, confirming a negative effect on niche function (Figure S6B).

We also asked whether the splenic niche, where mobilized HSPCs colonize, is altered in response to c-di-GMP. Indeed, although the microscopic architecture of the splenic niche was not deformed following c-di-GMP administration (Figure S6C), the number of non-hematopoietic cells significantly increased in the spleen (Figures S6D and S6E).

#### Signaling via TGF- $\beta$ and G-CSF Is Essential for c-di-GMP-Dependent HSPC Expansion in the Spleen

To define the downstream targets of c-di-GMP, we performed GSEA of cDNA microarray data obtained from c-di-GMP-treated or non-treated MSCs. TGF- $\beta$  signaling, as well as type I IFN, NF- $\kappa$ B, p38 MAPK, and fibroblast growth factor (FGF) signaling, was upregulated (Figures 7A and S7A). In addition, phosphorylation of ERK1/2 and AKT, which are downstream targets of FGF, was not altered in MSCs after c-di-GMP treatment (Figure S7C). Thus, we tested the effect of TGF- $\beta$  signaling on HSPCs by c-di-GMP. TGF- $\beta$  promotes osteoblastic differentiation through phosphorylation of Smad2 and Smad3 (Chen et al., 2012). Accordingly, mRNAs encoding osteoblastic transcription factors were invariably upregulated in c-di-GMP-treated MSCs, whereas adipogenesis-related genes were downregulated (Figures 7B and S7B).

Smad2 exhibited focal activation in steady-state conditions as previously reported (Brenet et al., 2013), while phospho-Smad2 was globally upregulated after c-di-GMP treatment (Figures 7C and 7D), an effect observed in *Irfnar1*<sup>-/-</sup> and *Irf3*<sup>-/-</sup>:*Irf7*<sup>-/-</sup> mice (Figure S7D). Although TGF- $\beta$  alone was not sufficient to alter HSPC dynamics in the BM and spleen (Figures S7E–S7G), TGF- $\beta$  receptor 1 inhibition decreased MPPs in the spleen upon c-di-GMP treatment, albeit with no obvious change in BM HSPCs (Figures 7E–7G). We

conclude that TGF- $\beta$  signaling is essential for HSPC expansion in the spleen but does not alter the HSPC pool size in the BM.

We next sought to identify cytokines that stimulate BM HSPC function. Serum levels of G-CSF were increased in c-di-GMP-treated mice, whereas levels of other inflammatory cytokines were not (Figure S7H). Accordingly, c-di-GMP treatment reduced HSPC mobilization in G-CSF receptor-deficient mice (*Csf3r*<sup>-/-</sup>), whereas HSPC fractions in BM did not show similar effects (Figures S7I and S7J), suggesting that G-CSF is a c-di-GMP target. However, Smad2 phosphorylation was observed in *Csf3r*<sup>-/-</sup> mice (Figure S7D), suggesting that G-CSF and TGF- $\beta$  independently regulate HSPC expansion in the spleen.

#### DISCUSSION

In this study, we identified crucial roles for c-di-GMP/STING signaling in the dynamics of hematopoiesis through modulation of HSPCs and their niches. A previous observation that HPSC expansion under infectious stress occurs even in the absence of TLR signaling or type I IFN responses indicated that unknown bacteria-derived factors activate a signal that stimulates HSPC expansion (Scumpia et al., 2010). Our results suggest that c-di-GMP is a bacteria-derived activator of this expansion that acts via the induction of extramedullary hematopoiesis and modulation of the BM microenvironment through STING.

#### c-di-GMP/STING Signaling Induces MPP Expansion in the Periphery and Decreases the Number of LT-HSCs

c-di-GMP treatment decreased the number of various hematopoietic cells, including LT-HSCs, in vivo. Notably, c-di-GMP suppressed the reconstitution capacity and cell-cycle quiescence of LT-HSCs, whereas it substantially increased the MPP number in the spleen, an effect likely due to the mobilization and proliferation of MPPs. Although we could not calculate the precise number of MPPs in the BM due to potential contamination by the LKS<sup>-</sup> fraction, as it has been reported that the LKS<sup>-</sup> fraction can contaminate MPPs in BM for IFN-stimulated HSPCs (Pietras et al., 2014), the short-term reconstitution capacity was potentiated in splenic MPPs. This finding supports the idea that splenic HPSCs function to supply immune cells in peripheral tissues through cell division (Massberg et al., 2007).

In contrast to c-di-GMP treatment, the number of HSPCs in *STING*<sup>-/-</sup> mice subjected to CeLP was comparable to that in *STING*<sup>+/+</sup> mice, suggesting redundancy of signals downstream of STING and those activated by bacteria via Toll-like or NOD1 receptors (Burberry et al., 2014).

(C and D) *STING*<sup>+/+</sup> (WT) or *STING*<sup>-/-</sup> (KO) mice were intraperitoneally injected with PBS (Ctrl) or 200 nmol of c-di-GMP (cdG), and BM cells were analyzed by FACS 3 days later (mean  $\pm$  SD, n = 4 from two independent experiments). (C) The number of cells in the LSK-gated fraction of the BM. (D) The number of cells in the LSK-gated fraction of the spleen.

(E and F) *Irfnar1*<sup>+/+</sup> (WT) or *Irfnar1*<sup>-/-</sup> (KO) mice were intraperitoneally injected with PBS (Ctrl) or 200 nmol of c-di-GMP (cdG), and BM cells were analyzed by FACS 3 days later. (E) The number of cells in the LSK-gated fraction of the BM (mean  $\pm$  SD, n = 3–6 from two independent experiments). (F) The number of cells in the LSK-gated fraction of the spleen (mean  $\pm$  SD, n = 5–8 from three independent experiments).

\*p < 0.05, \*\*p < 0.01, and \*\*\*p < 0.001. n.s., not significant. See also Figure S4.

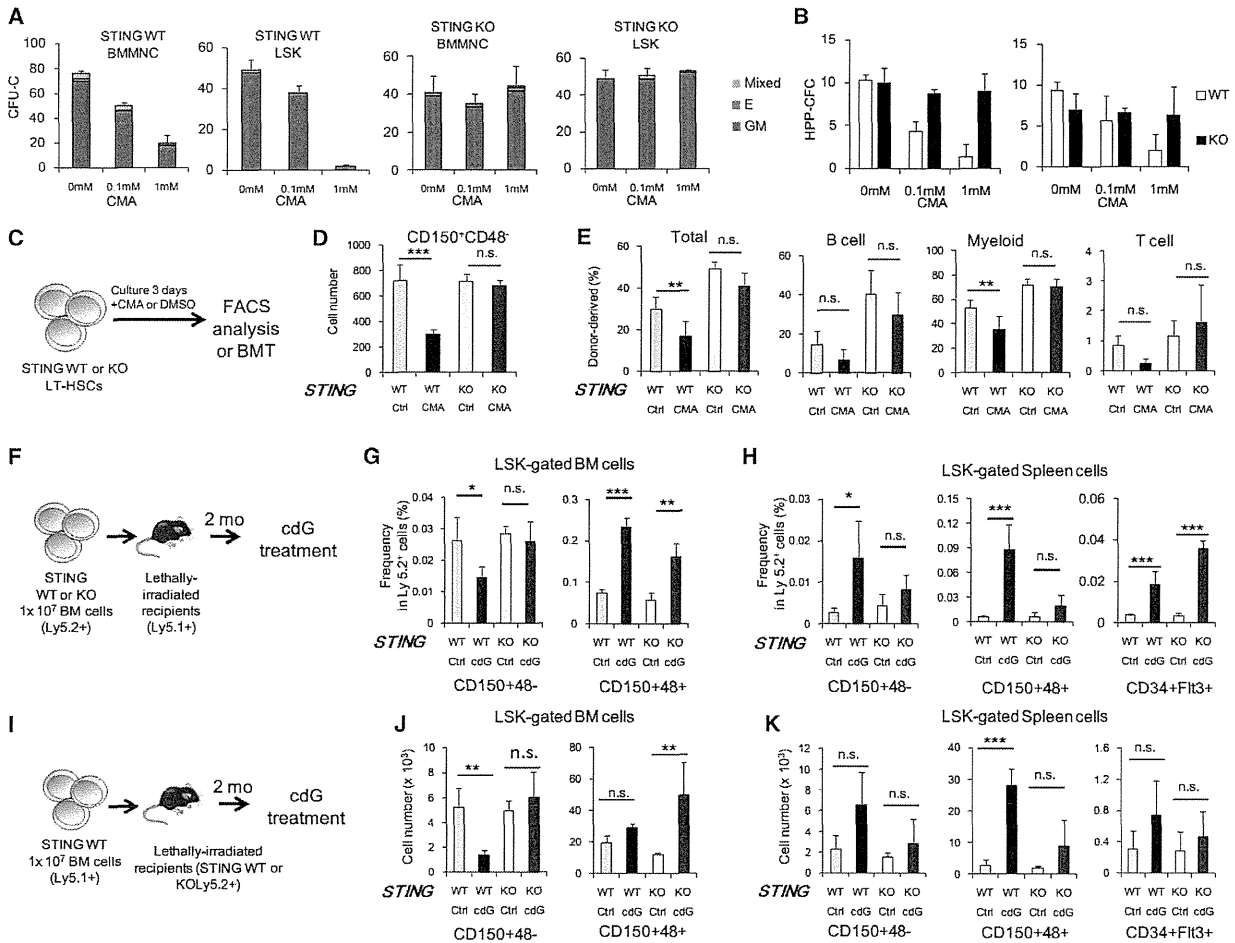


**Figure 5. STING Regulates HSPC Homeostasis in the BM and Spleen in Both Cell-Autonomous and Non-Cell-Autonomous Manners**

(A) CFU-Cs of  $1 \times 10^4$  BMMNCs or 150 LSK cells from *STING*<sup>+/+</sup> or *STING*<sup>-/-</sup> mice at the indicated CMA concentrations (mean  $\pm$  SD, n = 3).  
 (B) HPP-CFCs of BMMNC or LSK cells from *STING*<sup>+/+</sup> or *STING*<sup>-/-</sup> mice at the indicated CMA concentrations (mean  $\pm$  SD, n = 3).  
 (C) Experimental design for the repopulation assay of CMA-treated HSCs. In total, 500 (for transplantation) or 2,000 (for flow cytometry) CD34<sup>+</sup>Flt3<sup>-</sup> LSK cells from *STING*<sup>+/+</sup> or *STING*<sup>-/-</sup> mice were treated with DMSO or 1 mM CMA for 3 days and analyzed by FACS or transplanted into lethally irradiated mice.  
 (D) The number of CD150<sup>+</sup>CD41<sup>-</sup>CD48<sup>-</sup> LSK cells after 3 days of culture (mean  $\pm$  SD, n = 5–6).  
 (E) The frequency of donor-derived cells 1 month after BMT (mean  $\pm$  SD, n = 5–6).  
 (F) Experimental design for analysis shown in (G) and (H). Ly5.2<sup>+</sup> *STING*<sup>+/+</sup> (WT) or *STING*<sup>-/-</sup> (KO) donor cells were transplanted into Ly5.1<sup>+</sup> *STING*<sup>+/+</sup> recipient mice. Two months after BMT, mice were treated with PBS (Ctrl) or c-di-GMP (cdG), and the BM and spleen were analyzed 3 days later.  
 (G) The frequency of Ly5.2<sup>+</sup> cells in the LSK-gated fraction of the BM (mean  $\pm$  SD, n = 4).  
 (H) The frequency of Ly5.2<sup>+</sup> cells in the LSK-gated fraction of the spleen (mean  $\pm$  SD, n = 4).  
 (I) Experimental design for analysis shown in (J) and (K). Ly5.1<sup>+</sup> *STING*<sup>+/+</sup> BM cells were transplanted into Ly5.2<sup>+</sup> *STING*<sup>+/+</sup> (WT) or *STING*<sup>-/-</sup> (KO) recipients. Two months later, mice were treated with PBS (Ctrl) or c-di-GMP (cdG), and the BM and spleen were analyzed 3 days later.  
 (J) The number of LSK-gated cells in each indicated fraction of the BM (mean  $\pm$  SD, n = 4).  
 (K) The number of LSK-gated cells in each indicated fraction of the spleen (mean  $\pm$  SD, n = 4).  
 \*p < 0.05, \*\*p < 0.01, and \*\*\*p < 0.001. n.s., not significant. See also Figure S5.

### The *Ir3*/Type I IFN Axis Is a Bidirectional Regulator of HSPCs

Type I IFN signaling is a major downstream target of STING and an important response to infection that allows expansion of the HSPC pool size (Essers et al., 2009; Sato et al., 2009). In HSPCs, cell-cycle activation and mobilization are correlated to some extent (Tesio et al., 2013). Unexpectedly, how-

ever, we demonstrated that *Ir3*/type I IFN signaling inhibits phenotypic HSPC expansion in the spleen, suggesting that cell mobilization and proliferation are independently regulated in HSPCs, contrary to previous views. The literature suggests that both cell-autonomous and non-cell-autonomous mechanisms negatively regulate HSPCs. For example, type I IFN signaling reportedly suppresses HSC activation ex vivo

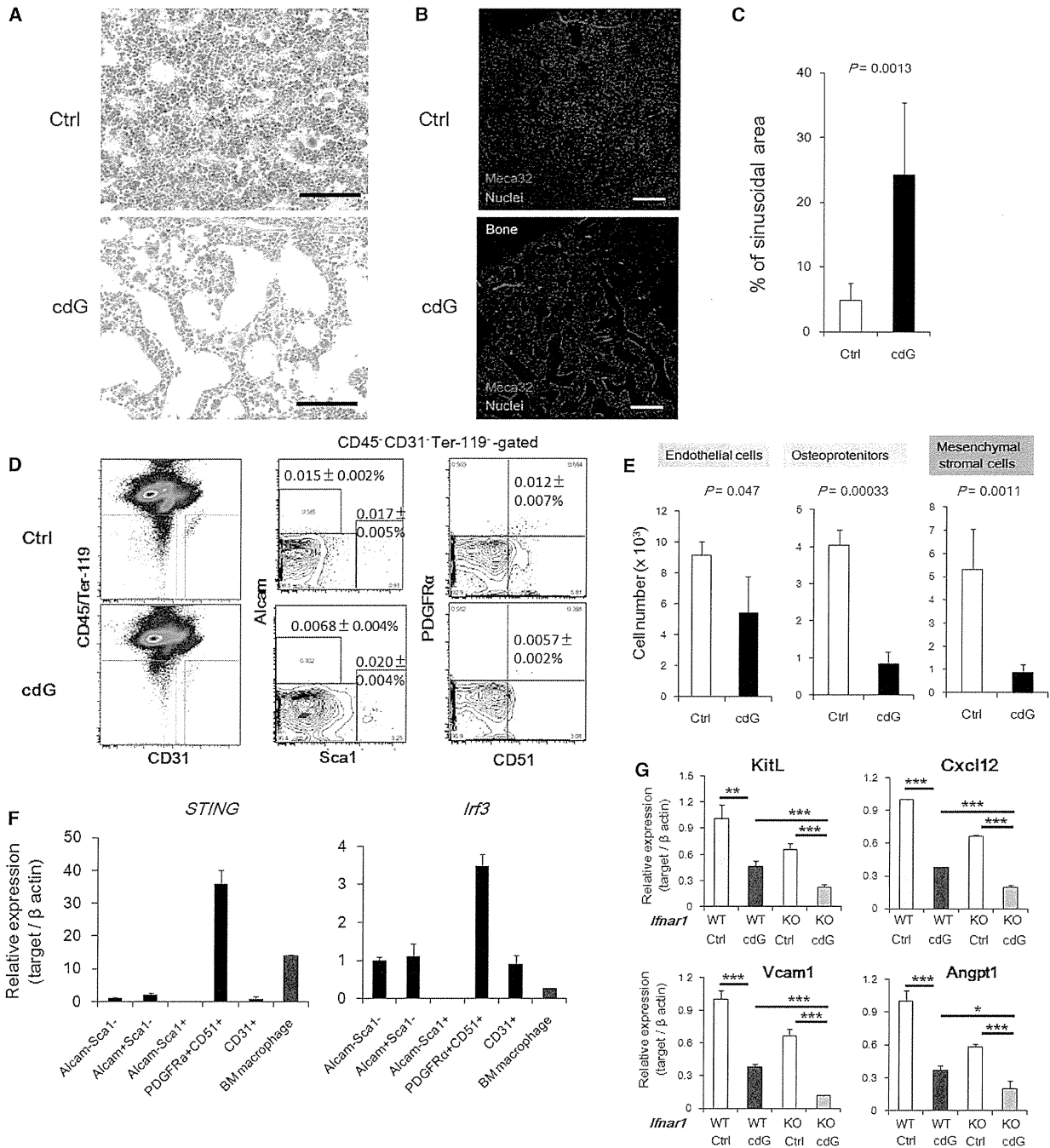


**Figure 6. c-di-GMP Attenuates MSC Function in the BM Niche**

(A) Mice were intraperitoneally injected with PBS (Ctrl) or 200 nmol of c-di-GMP (cdG). The femur was fixed 3 days later and stained with H&E. Scale bars indicate 100  $\mu$ m.

(B and C) Frozen sections of femur were stained with an anti-PLVAP monoclonal antibody (Meca32) and DAPI (nuclei). (B) Representative photomicrographs of femur sections. Scale bars indicate 100  $\mu$ m. (C) The proportion of the sinusoidal area in comparison to the entire BM area (mean  $\pm$  SD, n = 5–8; representative of three independent experiments).

(D and E) Mice were intraperitoneally injected with PBS (Ctrl, open bars) or 200 nmol of c-di-GMP (cdG, closed bars), and each indicated type of non-hematopoietic cells in the BM plug was analyzed 3 days later (mean  $\pm$  SD, n = 5). (D) Representative FACS plots of non-hematopoietic cells and the frequency among whole BM cells. (E) The number of cells in the indicated fractions.

(legend continued on next page)

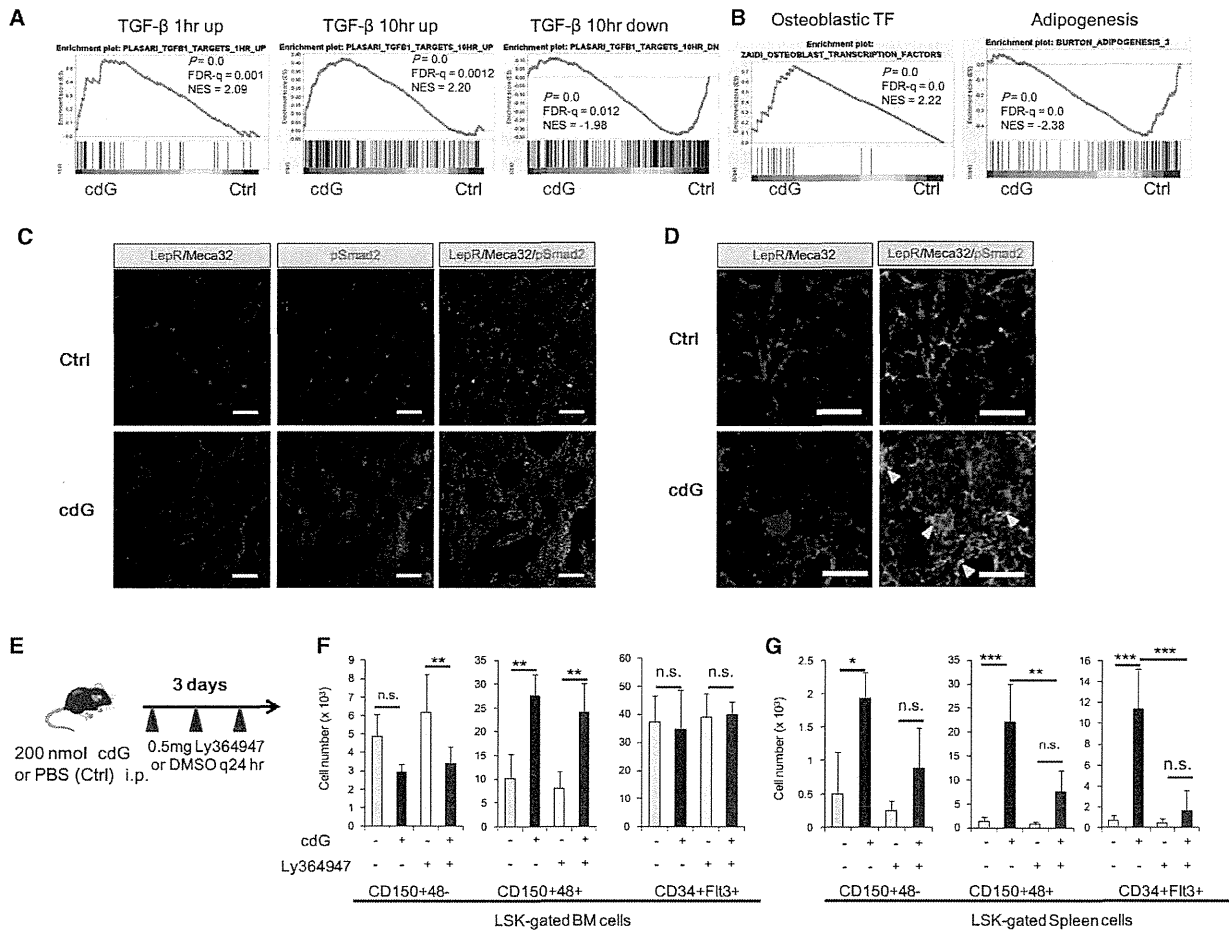


**Figure 7. c-di-GMP-Dependent TGF- $\beta$  Signaling Underlies Phenotypic HSPC Expansion in the Spleen**

(A and B) GSEA was performed using cDNA microarray data of MSCs (CD45<sup>+</sup>Ter-119<sup>-</sup>CD31<sup>-</sup>PDGFR $\alpha$ <sup>+</sup>CD51<sup>+</sup> cells) from PBS- or c-di-GMP-treated mice. FDR-q, false discovery rate. NES, normalized enrichment score. (A) Results for gene sets of the TGF- $\beta$  signaling pathway. (B) Results for gene sets of osteoblastic transcription factors and adipogenesis-related genes.

(C and D) Immunohistochemical analysis of phospho-Smad2 in the BM upon c-di-GMP treatment. PBS (Ctrl) or 200 nmol of c-di-GMP (cdG) was intraperitoneally administered and BM sections were stained with anti-leptin receptor (LepR), anti-PLVAP (Meca32), and anti-Smad2 phospho-specific (pSmad2) antibodies. (C) Lower-magnification images. Scale bar indicates 50  $\mu$ m. (D) Higher-magnification image of the area around a sinusoid. Arrowheads indicate LepR<sup>+</sup>/pSmad2<sup>+</sup> cells. Scale bar indicates 20  $\mu$ m.

(E) Experimental design of TGF- $\beta$  inhibition. PBS (Ctrl) or 200 nmol of c-di-GMP (cdG) was intraperitoneally administered, followed by daily administration of DMSO or 0.5 mg of Ly364947 for 3 days (n = 3–4, mean  $\pm$  SD).

(F) The number of cells in the LSK fraction of the BM.

(G) The number of cells in the LSK fraction of the spleen.

\*p < 0.05, \*\*p < 0.01, and \*\*\*p < 0.001. n.s., not significant. See also Figure S7.

(Pietras et al., 2014; Verma et al., 2002), an activity that requires p38 MAPK activation in part. Another possible mechanism is upregulation of a systemic inflammatory response. *Irf3* reportedly interferes with expression of the p40 subunit of interleukin (IL)-12, thereby limiting T helper type 1 cell (TH1)

and IL-17-producing helper T cell (TH17) activation upon viral infection (Negishi et al., 2012). Thus, in turn, c-di-GMP treatment may have augmented a systemic inflammatory response in *Irf3*<sup>-/-</sup>, *Irf3*<sup>-/-</sup>:*Irf1*<sup>-/-</sup>, and *Irfar1*<sup>-/-</sup> mice (Sato et al., 2009).

(F) Expression levels of *STING* (left) and *Irf3* (right) in the indicated non-hematopoietic fractions (mean  $\pm$  SD, n = 4).

(G) The fold differences in expression levels (by qPCR analysis) of the indicated genes in MSCs (CD45<sup>+</sup>Ter-119<sup>-</sup>CD31<sup>-</sup>PDGFR $\alpha$ <sup>+</sup>CD51<sup>+</sup> cells) in c-di-GMP-compared to PBS-treated *Irfar1*<sup>+/+</sup> (WT) or *Irfar1*<sup>-/-</sup> (KO) mice (mean  $\pm$  SD, n = 4).

\*p < 0.05, \*\*p < 0.01, and \*\*\*p < 0.001. n.s., not significant. See also Figure S6.



### c-di-GMP/STING Signaling Modulates Hematopoietic Niches

Although previous studies have focused primarily on the effect of inflammatory signals on HSPCs themselves (King and Goodell, 2011), our observations suggest the importance of niche cells in response to infectious stress. HSPCs are mobilized to infection sites (Massberg et al., 2007); therefore, facilitating their egress from the BM by niche modification is a reasonable defense mechanism against infection. Others have proposed that egress is induced by the degradation of CXCR4 in HSPCs and CXCL12 in niche cells (Lévesque et al., 2003). CD8<sup>+</sup> T cells were recently shown to play a role in HSPC stimulation by promoting cytokine release from MSCs (Schürch et al., 2014). However, this mechanism cannot account for the c-di-GMP-mediated response, because BM chimeras with *STING*<sup>-/-</sup> hematopoietic cells and *STING*<sup>+/+</sup> niche cells still show MPP expansion in the BM and CD34<sup>+</sup>Fit3<sup>+</sup> LSK cell expansion in the spleen. MSCs show the highest STING expression among niche cells; therefore, we propose that c-di-GMP has detrimental effects on the ability of MSCs to control HSC number and maintain their function, likely through upregulating TGF- $\beta$  signaling, as discussed below. Loss of HSPC niche factors in the BM is required for egress of these cells from the BM sinusoidal network and to promote an inter-BM exchange of HSPCs, as well as to supply immune cells to the periphery.

### TGF- $\beta$ Signaling Is Essential for MPP Expansion in the Spleen by c-di-GMP/STING Signaling

TGF- $\beta$  maintains HSC function in a steady state (Yamazaki et al., 2011) and facilitates restoration of HSC quiescence under stress conditions (Brenet et al., 2013). We demonstrated that TGF- $\beta$  activation is also required for HSPC expansion in the spleen following c-di-GMP treatment, an effect presumably due to altered MSC function.

TGF- $\beta$  treatment alone had a minimal mobilizing effect on HSPCs compared with activation of type I IFN, NF- $\kappa$ B, or p38 MAPK, downregulation of Notch activity, or G-CSF overproduction. Nonetheless, TGF- $\beta$  activity may cooperate with these factors to alter HSPC number and/or function through c-di-GMP-STING signaling. Given the global upregulation of TGF- $\beta$  in the BM following c-di-GMP treatment independent of G-CSF signaling, we do not exclude the possibility that TGF- $\beta$  activates a mechanism intrinsic to HSPCs that promotes their mobilization, although gene expression profile data do not support this conclusion.

This study reports how the bacteria-derived molecule c-di-GMP governs HSPC dynamics following infection independent of TLR and IFN signaling. c-di-GMP/STING signaling activates various pathways in multiple cell types, including type I IFN signaling and alteration of MSC function, to efficiently expand and relocalize hematopoietic precursors, which would modulate a robust response of HSPCs to bacterial infection. c-di-GMP promotes cell-cycle entry and HSC mobilization; therefore, a c-di-GMP mimetic or STING agonist could act as a novel HSPC modulator. Further investigation of the activity and regulation of c-di-GMP and its downstream signals should benefit our understanding of the relationship between the pathophysiology of bacterial infection and HSPC dynamics.

### EXPERIMENTAL PROCEDURES

#### Mice

C57BL/6J mice (8–12 weeks old) were used in all experiments, unless otherwise stated. C57BL/6-Ly5.1 congenic mice were used for competitive repopulation assays. *Irf3*-deficient mice and *Irf3/Irf7*-deficient mice (Honda et al., 2005) were kindly provided by Dr. Tadatsugu Taniguchi (University of Tokyo). STING-deficient mice (Ishikawa and Barber, 2008) were kindly provided by Dr. Takashi Saito (RIKEN) with the permission of Dr. Glen Barber (University of Miami). IFNAR1-deficient mice (Müller et al., 1994) were purchased from The Jackson Laboratory. *Evi1*-GFP reporter mice (Kataoka et al., 2011) were provided by Dr. Mineo Kurokawa (University of Tokyo). Ubc-GFP reporter mice (Schaefer et al., 2001) were purchased from The Jackson Laboratory. CSF3R-deficient mice (Liu et al., 1996) were provided by Dr. Shinsuke Yuasa (Keio University). All procedures were performed in accordance with the guidelines of Keio University School of Medicine. For detailed methods, see Supplemental Experimental Procedures.

#### ACCESSION NUMBERS

The GEO accession number for the microarray data used in this study is GSE65905.

#### SUPPLEMENTAL INFORMATION

Supplemental Information includes Supplemental Experimental Procedures and seven figures and can be found with this article online at <http://dx.doi.org/10.1016/j.celrep.2015.02.066>.

#### AUTHOR CONTRIBUTIONS

H.K., K.T., C.I.K., A.N.-I., and D.K. performed the experiments. H.K., K.T., H.H., and K.N.Y. analyzed the results. T. Sato, T.O., Y.H., G.N.B., and M.K. provided scientific advice and materials. H.K. and K.T. wrote the manuscript. K.T. and T. Suda conceived the project and supervised the research.

#### ACKNOWLEDGMENTS

We thank T. Taniguchi and H. Negishi for providing *Irf3*<sup>-/-</sup> and *Irf3*<sup>-/-</sup>:*Irf7*<sup>-/-</sup> mice; A. Shibuya and N. Totsuka for advice on the CeLP procedure; M. Suematsu and T. Hishiki for fluorescence-activated cell sorting analysis and c-di-GMP characterization; T. Muraki, K. Endo, M. Katabami-Maie, and T. Hirose for technical support and laboratory management; and R. Goitsuka for providing mice. K.T. was supported by the Tenure-Track Program at the Sakauchi Laboratory and in part by a MEXT Grant-in-Aid for Young Scientists (A), a grant from the National Center for Global Health and Medicine, and a grant from the Japan Science and Technology Agency (JST), Core Research for Evolution Science and Technology (CREST). T. Suda and K.T. were supported in part by a MEXT Grant-in-Aid for Scientific Research (A) and a MEXT Grant-in-Aid for Scientific Research on Innovative Areas. H.K., C.I.K., and A.N.-I. are research fellows of the Japan Society for the Promotion of Science.

Received: November 11, 2014

Revised: January 22, 2015

Accepted: February 28, 2015

Published: April 2, 2015

#### REFERENCES

- Ablasser, A., Goldeck, M., Cavlar, T., Deimling, T., Witte, G., Röhl, I., Hopfner, K.P., Ludwig, J., and Hornung, V. (2013). cGAS produces a 2'-5'-linked cyclic dinucleotide second messenger that activates STING. *Nature* **498**, 380–384.
- Blanpain, C., Mohrin, M., Sotriopoulou, P.A., and Passegué, E. (2011). DNA-damage response in tissue-specific and cancer stem cells. *Cell Stem Cell* **8**, 16–29.

- Brenet, F., Kermani, P., Spektor, R., Rafii, S., and Scandura, J.M. (2013). TGF $\beta$  restores hematopoietic homeostasis after myelosuppressive chemotherapy. *J. Exp. Med.* *210*, 623–639.
- Burberry, A., Zeng, M.Y., Ding, L., Wicks, I., Inohara, N., Morrison, S.J., and Núñez, G. (2014). Infection mobilizes hematopoietic stem cells through cooperative NOD-like receptor and Toll-like receptor signaling. *Cell Host Microbe* *15*, 779–791.
- Burdette, D.L., Monroe, K.M., Sotelo-Troha, K., Iwig, J.S., Eckert, B., Hyodo, M., Hayakawa, Y., and Vance, R.E. (2011). STING is a direct innate immune sensor of cyclic di-GMP. *Nature* *478*, 515–518.
- Cavlar, T., Deimling, T., Ablasser, A., Hopfner, K.P., and Hornung, V. (2013). Species-specific detection of the antiviral small-molecule compound CMA by STING. *EMBO J.* *32*, 1440–1450.
- Challen, G.A., Boles, N.C., Chambers, S.M., and Goodell, M.A. (2010). Distinct hematopoietic stem cell subtypes are differentially regulated by TGF- $\beta$ 1. *Cell Stem Cell* *6*, 265–278.
- Chen, G., Deng, C., and Li, Y.P. (2012). TGF- $\beta$  and BMP signaling in osteoblast differentiation and bone formation. *Int. J. Biol. Sci.* *8*, 272–288.
- Crane, J.L., and Cao, X. (2014). Bone marrow mesenchymal stem cells and TGF- $\beta$  signaling in bone remodeling. *J. Clin. Invest.* *124*, 466–472.
- Essers, M.A., Offner, S., Blanco-Bose, W.E., Waibler, Z., Kalinke, U., Duchosal, M.A., and Trumpp, A. (2009). IFN $\alpha$  activates dormant haematopoietic stem cells in vivo. *Nature* *458*, 904–908.
- Hengge, R. (2009). Principles of c-di-GMP signalling in bacteria. *Nat. Rev. Microbiol.* *7*, 263–273.
- Honda, K., and Taniguchi, T. (2006). IRFs: master regulators of signalling by Toll-like receptors and cytosolic pattern-recognition receptors. *Nat. Rev. Immunol.* *6*, 644–658.
- Honda, K., Yanai, H., Negishi, H., Asagiri, M., Sato, M., Mizutani, T., Shimada, N., Ohba, Y., Takaoka, A., Yoshida, N., and Taniguchi, T. (2005). IRF-7 is the master regulator of type-I interferon-dependent immune responses. *Nature* *434*, 772–777.
- Ishikawa, H., and Barber, G.N. (2008). STING is an endoplasmic reticulum adaptor that facilitates innate immune signalling. *Nature* *455*, 674–678.
- Karaolis, D.K., Means, T.K., Yang, D., Takahashi, M., Yoshimura, T., Muraille, E., Philpott, D., Schroeder, J.T., Hyodo, M., Hayakawa, Y., et al. (2007). Bacterial c-di-GMP is an immunostimulatory molecule. *J. Immunol.* *178*, 2171–2181.
- Kataoka, K., Sato, T., Yoshimi, A., Goyama, S., Tsuruta, T., Kobayashi, H., Shimabe, M., Arai, S., Nakagawa, M., Imai, Y., et al. (2011). Evi1 is essential for hematopoietic stem cell self-renewal, and its expression marks hematopoietic cells with long-term multilineage repopulating activity. *J. Exp. Med.* *208*, 2403–2416.
- Keller, H., Yunxu, C., Marit, G., Pla, M., Reiffers, J., Thèze, J., and Froussard, P. (1999). Transgene expression, but not gene delivery, is improved by adhesion-assisted lipofection of hematopoietic cells. *Gene Ther.* *6*, 931–938.
- King, K.Y., and Goodell, M.A. (2011). Inflammatory modulation of HSCs: viewing the HSC as a foundation for the immune response. *Nat. Rev. Immunol.* *11*, 685–692.
- Lévesque, J.P., Hendy, J., Takamatsu, Y., Simmons, P.J., and Bendall, L.J. (2003). Disruption of the CXCR4/CXCL12 chemotactic interaction during hematopoietic stem cell mobilization induced by G-CSF or cyclophosphamide. *J. Clin. Invest.* *111*, 187–196.
- Liu, F., Wu, H.Y., Wesselschmidt, R., Kornaga, T., and Link, D.C. (1996). Impaired production and increased apoptosis of neutrophils in granulocyte colony-stimulating factor receptor-deficient mice. *Immunity* *5*, 491–501.
- Massberg, S., Schaefer, P., Knezevic-Maramica, I., Köllnberger, M., Tubo, N., Moseman, E.A., Huff, I.V., Junt, T., Wagers, A.J., Mazo, I.B., and von Andrian, U.H. (2007). Immunosurveillance by hematopoietic progenitor cells trafficking through blood, lymph, and peripheral tissues. *Cell* *131*, 994–1008.
- McWhirter, S.M., Barbalat, R., Monroe, K.M., Fontana, M.F., Hyodo, M., Joncker, N.T., Ishii, K.J., Akira, S., Colonna, M., Chen, Z.J., et al. (2009). A host type I interferon response is induced by cytosolic sensing of the bacterial second messenger cyclic-di-GMP. *J. Exp. Med.* *206*, 1899–1911.
- Méndez-Ferrer, S., Michurina, T.V., Ferraro, F., Mazloom, A.R., Macarthur, B.D., Lira, S.A., Scadden, D.T., Ma'ayan, A., Enikolopov, G.N., and Frenette, P.S. (2010). Mesenchymal and haematopoietic stem cells form a unique bone marrow niche. *Nature* *466*, 829–834.
- Müller, U., Steinhoff, U., Reis, L.F., Hemmi, S., Pavlovic, J., Zinkernagel, R.M., and Aguet, M. (1994). Functional role of type I and type II interferons in antiviral defense. *Science* *264*, 1918–1921.
- Nagai, Y., Garrett, K.P., Ohta, S., Bahrun, U., Kouro, T., Akira, S., Takatsu, K., and Kinrade, P.W. (2006). Toll-like receptors on hematopoietic progenitor cells stimulate innate immune system replenishment. *Immunity* *24*, 801–812.
- Negishi, H., Yanai, H., Nakajima, A., Koshiba, R., Atarashi, K., Matsuda, A., Matsuki, K., Miki, S., Doi, T., Aderem, A., et al. (2012). Cross-interference of RLR and TLR signaling pathways modulates antibacterial T cell responses. *Nat. Immunol.* *13*, 659–666.
- Omatsu, Y., Sugiyama, T., Kohara, H., Kondoh, G., Fujii, N., Kohno, K., and Nagasawa, T. (2010). The essential functions of adipo-osteogenic progenitors as the hematopoietic stem and progenitor cell niche. *Immunity* *33*, 387–399.
- Orkin, S.H., and Zon, L.I. (2008). Hematopoiesis: an evolving paradigm for stem cell biology. *Cell* *132*, 631–644.
- Pietras, E.M., Lakshminarasimhan, R., Techner, J.M., Fong, S., Flach, J., Binnewies, M., and Passegué, E. (2014). Re-entry into quiescence protects hematopoietic stem cells from the killing effect of chronic exposure to type I interferons. *J. Exp. Med.* *211*, 245–262.
- Pinho, S., Lacombe, J., Hanoun, M., Mizoguchi, T., Bruns, I., Kunisaki, Y., and Frenette, P.S. (2013). PDGFR $\alpha$  and CD51 mark human nestin+ sphere-forming mesenchymal stem cells capable of hematopoietic progenitor cell expansion. *J. Exp. Med.* *210*, 1351–1367.
- Rittirsch, D., Huber-Lang, M.S., Flierl, M.A., and Ward, P.A. (2009). Immunodysregulation of experimental sepsis by cecal ligation and puncture. *Nat. Protoc.* *4*, 31–36.
- Sato, T., Onai, N., Yoshihara, H., Arai, F., Suda, T., and Ohteki, T. (2009). Interferon regulatory factor-2 protects quiescent hematopoietic stem cells from type I interferon-dependent exhaustion. *Nat. Med.* *15*, 696–700.
- Schaefer, B.C., Schaefer, M.L., Kappler, J.W., Marrack, P., and Kedl, R.M. (2001). Observation of antigen-dependent CD8+ T-cell/dendritic cell interactions in vivo. *Cell. Immunol.* *214*, 110–122.
- Schürch, C.M., Riether, C., and Ochsnein, A.F. (2014). Cytotoxic CD8+ T cells stimulate hematopoietic progenitors by promoting cytokine release from bone marrow mesenchymal stromal cells. *Cell Stem Cell* *14*, 460–472.
- Scumpia, P.O., Kelly-Scumpia, K.M., Delano, M.J., Weinstein, J.S., Cuenca, A.G., Al-Quran, S., Bovio, I., Akira, S., Kumagai, Y., and Moldawer, L.L. (2010). Cutting edge: bacterial infection induces hematopoietic stem and progenitor cell expansion in the absence of TLR signaling. *J. Immunol.* *184*, 2247–2251.
- Tesio, M., Oser, G.M., Baccelli, I., Blanco-Bose, W., Wu, H., Göthert, J.R., Kogan, S.C., and Trumpp, A. (2013). Pten loss in the bone marrow leads to G-CSF-mediated HSC mobilization. *J. Exp. Med.* *210*, 2337–2349.
- Verma, A., Deb, D.K., Sassano, A., Uddin, S., Varga, J., Wickrema, A., and Plataniias, L.C. (2002). Activation of the p38 mitogen-activated protein kinase mediates the suppressive effects of type I interferons and transforming growth factor- $\beta$  on normal hematopoiesis. *J. Biol. Chem.* *277*, 7726–7735.
- Yamazaki, S., Ema, H., Karlsson, G., Yamaguchi, T., Miyoshi, H., Shioda, S., Taketo, M.M., Karlsson, S., Iwama, A., and Nakauchi, H. (2011). Nonmyelinating Schwann cells maintain hematopoietic stem cell hibernation in the bone marrow niche. *Cell* *147*, 1146–1158.
- Zhong, B., Yang, Y., Li, S., Wang, Y.Y., Li, Y., Diao, F., Lei, C., He, X., Zhang, L., Tien, P., and Shu, H.B. (2008). The adaptor protein MIRA links virus-sensing receptors to IRF3 transcription factor activation. *Immunity* *29*, 538–550.
- Zhou, B.O., Yue, R., Murphy, M.M., Peyer, J.G., and Morrison, S.J. (2014). Leptin-receptor-expressing mesenchymal stromal cells represent the main source of bone formed by adult bone marrow. *Cell Stem Cell* *15*, 154–168.

12 腫瘍

## 2. 組織球症

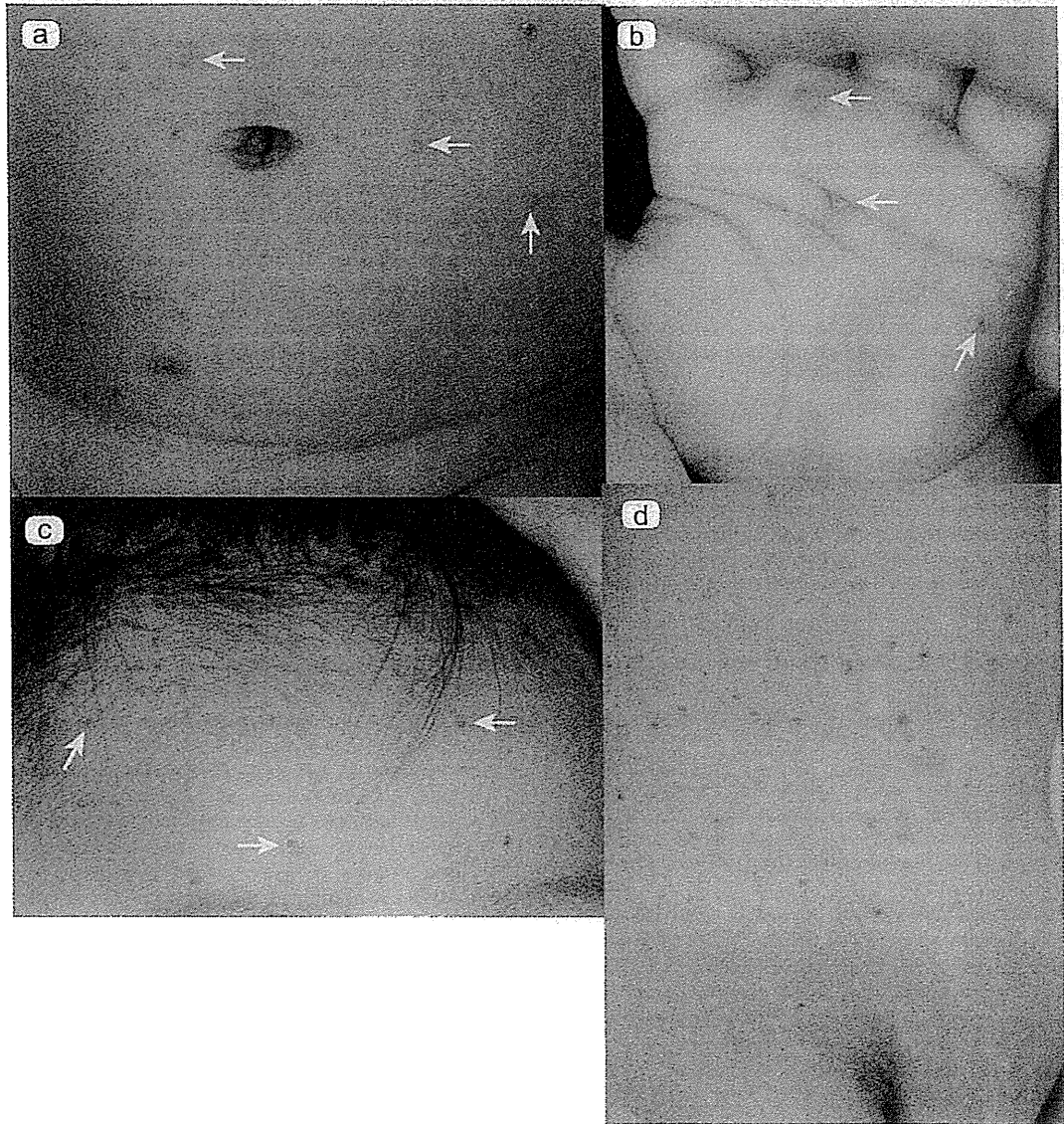
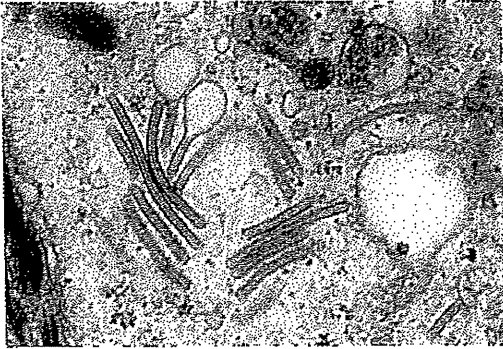


図1 ランゲルハンス細胞組織球症 (LCH) の女児の臨床像

生後3週間より体幹, 前額, 手掌等に水疱出現。生後約3カ月時に当科(大阪大学皮膚科)受診(a~d)。ステロイド外用にても軽快せず, 前額部の水疱はむしろ悪化(c)。体幹部は一部白斑も混じる(d)。生後約4カ月より両耳下腺部のリンパ節腫脹, 脾腫出現。5カ月より熱発, 貧血出現したためビンブラスチン・プレドニゾンにて加療。1歳6カ月で骨髄移植。以後経過良好である。



② LCHの男児皮膚より生検した組織の電子顕微鏡像  
胞体内にラケット状のBirbeck顆粒を認める。

## 1. 組織球症とは

ランゲルハンス細胞などの樹状細胞やマクロファージがモノクローナルに増殖する疾患。皮膚、骨(頭蓋骨, 長管骨等), リンパ節, 肺, 肝, 脾などの造血系, 口腔粘膜, 胃腸粘膜, 胸腺, 甲状腺, 膵臓, 腎臓, 下垂体, 眼窩, 中枢神経系などさまざまな臓器に浸潤する。以下のように分類<sup>1)</sup>。

### ① ランゲルハンス細胞組織球症 (Langerhans cell histiocytosis : LCH)

I : LCH-SS : 単系統 (好酸球性肉芽腫症 : 多巣性骨病変)

II : LCH-MS : 多系統で重要臓器(-) (Hand-Schüller-Christian 病 : 2 ~ 5 歳で発症し骨病変, 眼球突出, 尿崩症を3徴候)

III : LCH-MS(RO) : 多系統で重要臓器(肝, 肺, 脾, 骨髄)を含む (Letterer-Siwe 病 : 2 歳未満で発症し多臓器に及ぶ)

② non-LCH : マクロファージの増殖による (若年性黄色腫, Rosai Dorfman 病, Erdheim-Chester 病)

③ 悪性組織球症

## 2. 診断のポイント (以下 LCH について述べる)

初発症状は皮膚が多い。丘疹, 水疱, びらん, 結節, 紫斑, とくに白斑など多彩な皮疹がさまざまな部位に出現するが<sup>2)</sup>, 非特異的な症状であるため早期診断が困難である<sup>3)</sup>。皮膚生検で診断する。免疫学的染色にて CD1a(+), CD207(langerin)(+)。電子顕微鏡にて胞体内にラケット状の Birbeck 顆粒を認める<sup>4)</sup>。

## 3. 検査

超音波検査 (肝脾腫, リンパ節腫大), 血液検査 (貧血, 血小板減少, バソプレシン濃度低下), X-P (頭蓋骨, 長管骨), MRI, 骨髄穿刺, 呼吸機能<sup>5)</sup>。

## 4. 治療

限局性の皮膚病変に対しては局所ステロイド外用を行う。LCH-MS 例に限り以前はビンブラスチン・プレドニゾロンが用いられていたが, 最近では LCH の原因遺伝子の一つは *BRAF* と考えられており, これに対して海外で vemurafenib (2014 年 12 月現在国内未承認) 等による治療も試みられている<sup>6)</sup>。骨髄移植が行われることもある<sup>5)</sup>。 (村上有香子)

